Preprint Title	Synthesis of photo- and ionochromic *N*-acylated 2-aminomethylenebenzo[*b*]thiophene-3(2*H*)-ones with a terminal phenanthroline group
Authors	Vladimir P. Rybalkin, Sofiya Y. Zmeeva, Lidiya L. Popova, Irina V. Dubonosova, Olga Y. Karlutova, Oleg P. Demidov, Alexander D. Dubonosov and Vladimir A. Bren
Publication Date	14 Nov 2023
Article Type	Full Research Paper
Supporting Information File 1	Supporting Information File 2.docx; 3.7 MB
Supporting Information File 2	Supporting Information File 3.docx; 469.4 KB
Supporting Information File 3	Supporting+Information+File+1.docx; 35.7 KB
ORCID® iDs	Vladimir P. Rybalkin - https://orcid.org/0000-0001-9327-1472; Sofiya Y. Zmeeva - https://orcid.org/0000-0002-0428-1087; Lidiya L. Popova - https://orcid.org/0009-0008-3021-7397; Irina V. Dubonosova - https://orcid.org/0000-0002-3368-5259; Olga Y. Karlutova - https://orcid.org/0000-0002-3290-101X; Oleg P. Demidov - https://orcid.org/0000-0002-3586-0487; Alexander D. Dubonosov - https://orcid.org/0000-0003-4701-2271; Vladimir A. Bren - https://orcid.org/0000-0003-3192-6204

Synthesis of photo- and ionochromic *N*-acylated 2-aminomethylenebenzo[*b*]thiophene-3(2*H*)-ones with a terminal phenanthroline group

Vladimir P. Rybalkin[1], Sofiya Yu. Zmeeva[2], Lidiya L. Popova[2], Irina V. Dubonosova[2], Olga Yu. Karlutova[2], Oleg P. Demidov[3], Alexander D. Dubonosov[*1]

and Vladimir A. Bren[2]

Address: [1]Federal Research Centre the Southern Scientific Centre of the Russian Academy of Sciences, Rostov-on-Don, 344006 Russian Federation, [2]Institute of Physical and Organic Chemistry, Southern Federal University, Rostov-on-Don, 344090 Russian Federation and [3]North Caucasus Federal University, 355009, Stavropol, Russian Federation

Email: Alexander D. Dubonosov[*] - aled@ipoc.sfedu.ru

* Corresponding author

Abstract

A series of *N*-acylated 2-aminomethylenebenzo[*b*]thiophene-3(2*H*)-ones with a terminal phenanthroline receptor substituent was synthesized. Upon irradiation in CH_3CN or DMSO with light of 436 nm, they undergo *Z/E* isomerization around the C=C bond followed by rapid N→O migration of the acyl group and the formation of non-emissive *O*-acylated isomers. These isomers were separated preparatively and fully characterized by IR, ^1H, ^{13}C NMR, HRMS and XRD methods. The reverse thermal reaction is catalyzed by protonic acids. *N*-Acylated compounds exclusively with Fe^{2+}

ions form non-fluorescent complexes with a contrast naked eye effect - color change of the solutions from yellow to pink-crimson. Subsequent selective interaction with acetate anions leads to the restoration of the initial absorption and emission spectra. Thus, the obtained compounds represent dual-mode “on-off-on” switches of optical and fluorescent properties under sequential exposure to light/H^+ or sequential addition of Fe^{2+}/AcO^- ions.

Keywords

acylated ketoenamines; photochromism; fluorescence; naked eye effect; molecular switches

Introduction

Photochromism is defined as the photoinduced reversible transformation of organic molecules between two forms that possess different absorption spectra [1-3]. Due to the difference in the structures of these states and the optical and emission properties, photochromic compounds are used in 3D optical memory devices, photoswitches of different types, molecular logic gates, photopharmacology, bioimaging and chemosensorics [4-10]. For most photochromic compounds, irradiation of their solutions or solids results in a deepening their color (positive photochromism). Less studied are those characterized by photoinduced bleaching (negative or inverse photochromism): merocyanine forms of spiropyrans and spirooxazines, azomethine imines, thioindigoid dyes and acylated ketoenamines [11-14]. Recently, they have been actively used to create next-generation molecular switches, materials with new properties (in particular, changing color depending on the intensity of sunlight), photochromic tags for biological research and optical sensors [11,15-20]. To develop

a new dual-mode molecular switches capable of effectively modulating optical and fluorescent properties both upon irradiation with visible light and upon sequential addition of Fe^{2+} cations and AcO^- anions, we synthesized 2-(*N*-acylaminomethylenebenzo)[*b*]thiophene-3(2*H*)-ones with terminal phenanthroline substituent and studied their spectral-luminescent, photochromic and ionochromic properties. The phenanthroline moiety was incorporated into the molecule due to its known ability to coordinate with metal cations [21,22].

Results and Discussion

N-Acylated 2-aminomethylenebenzo[*b*]thiophene-3(2*H*)-ones with terminal phenanthroline substituent **2a-c** were synthesized starting from 3-hydroxybenzo[*b*]thiophene-2-carbaldehyde according to Scheme 1 (Supporting Information File 1).

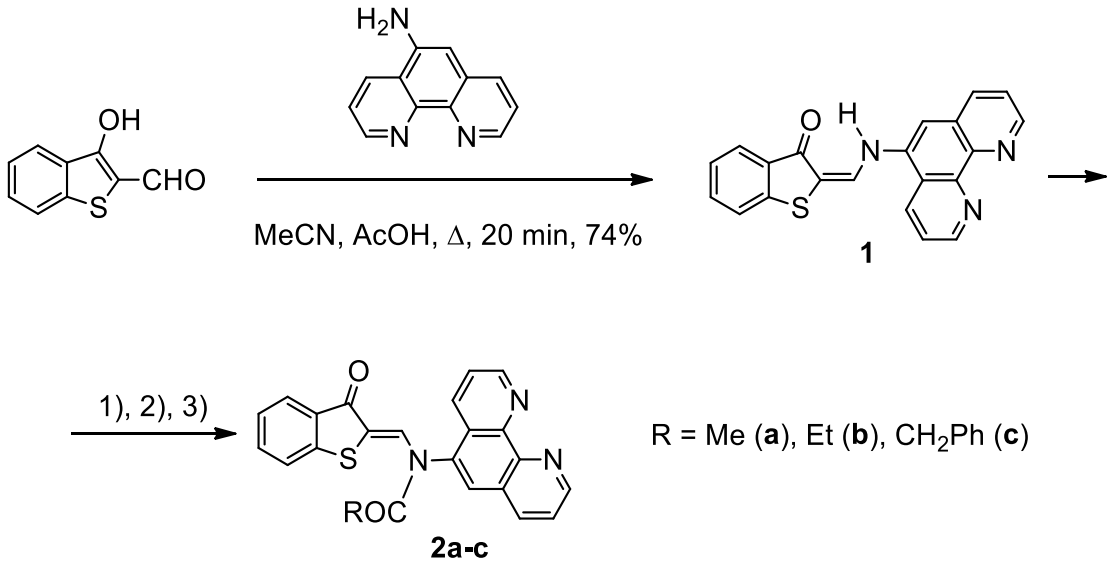

Scheme 1: Synthesis of ketoenamine **1** and *N*-acylated ketoenamines **2a-c**. 1) Compound **2a**, reagents and conditions: $(MeCO)_2O$, TEA, Δ, 89%; 2) Compound **2b**,

reagents and conditions: $(EtCO)_2O$, TEA, Δ, 83%; 3) Compound **2c**, reagents and conditions: MeCN, TEA, $PhCH_2COCl$, 68%.

The obtained compounds **2a–c** exist in the *N*-acylated keto form. In their IR spectra, stretching vibrations of the thiophene and amide carbonyl groups are observed at 1663-1678 and 1705-1713 cm^{-1}, respectively. The ^1H NMR spectra contain signals of methine protons =CH- in the region 7.92-9.02 ppm, which corresponds to the *Z*-configuration with respect to the C=C bond. According to data previously obtained [14], the signals of the methine protons of the *E*-isomers should be in the region of approximately 5.90 ppm [14]. Other IR, ^1H, ^{13}C NMR spectroscopy data and high-resolution mass spectrometry data confirming the structure of the synthesized compounds **1, 2a–c** are presented in Supporting Information File 2.

Non-acylated ketoenamine **1** shows long wavelength absorption at 458 nm, while acylation leads to a hypsochromic shift of this maximum in compounds **2a–c** to 423-426 nm (Table 1). The intensity of this absorption band decreases with increasing steric hindrance in the series R = acetyl (**2a**) > propionyl (**2b**) > phenylacetyl (**2c**).

Table 2: Absorption and fluorescence spectra of compounds **1, 2a, b** in acetonitrile and compound **2c** in DMSO[a].

Compound	λ_{abs}, nm (ε, L mol^{-1} cm^{-1})	λ_{fl}, nm (I_{fl}, rel. units)
1	344 (12800), 458 (20000)	506 (650)
2a	303 (25000), 423 (14000)	468 (790)
2b	300 (18800), 426 (9200)	465 (780)
2c	309 (24600), 425 (6800)	467 (710)

[a]λ_{abs}, λ_{fl} – the maxima of the absorption and fluorescence bands, respectively; I_{fl} – the relative fluorescence intensity; *c* 5.0 × 10^{-5} mol L^{-1}, λ_{ex} 420 nm (455 nm for **1**), PMT voltage 800 V.

N-Acylated ketoenamines **2a–c** in solutions exhibit fluorescence in the region of 465-468 nm, and the excitation emission spectra agree well with the absorption spectra (Figure 1).

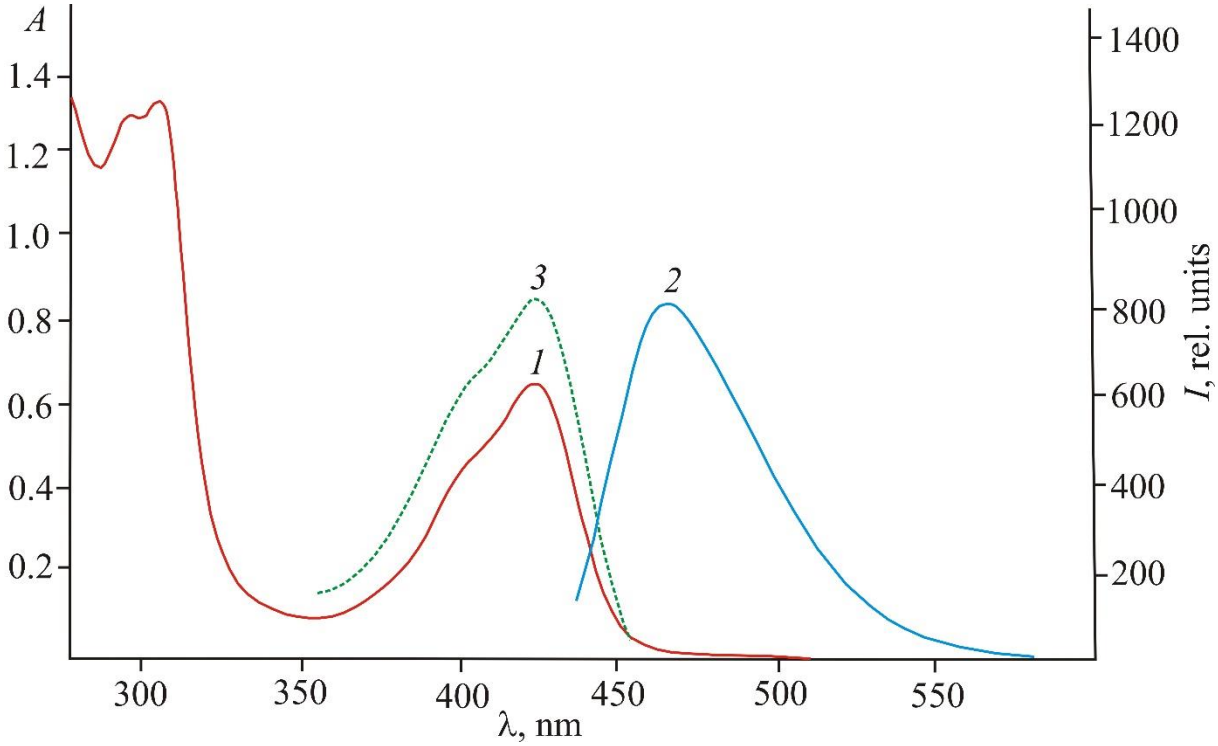

Figure 1: Absorption (*1*), fluorescence (λ_{ex} = 422 nm) (*2*) and fluorescence excitation (λ_{fl} = 465 nm) (*3*) spectra of compound **2a** in acetonitrile (*c* 5.0 × 10^{-5} mol L^{-1}).

Compounds **2a–c** in solutions demonstrate negative photochromic properties when irradiated with visible light of 436 nm (Figure 2). A decrease in the long-wavelength absorption is accompanied by a simultaneous increase in the absorption at the shorter wavelength spectral region 370 nm. During the photo process, a gradual diminishment

of the initial fluorescence intensity at 465-468 nm up to zero is observed. The resulting *O*-acylated isomers are non-emissive.

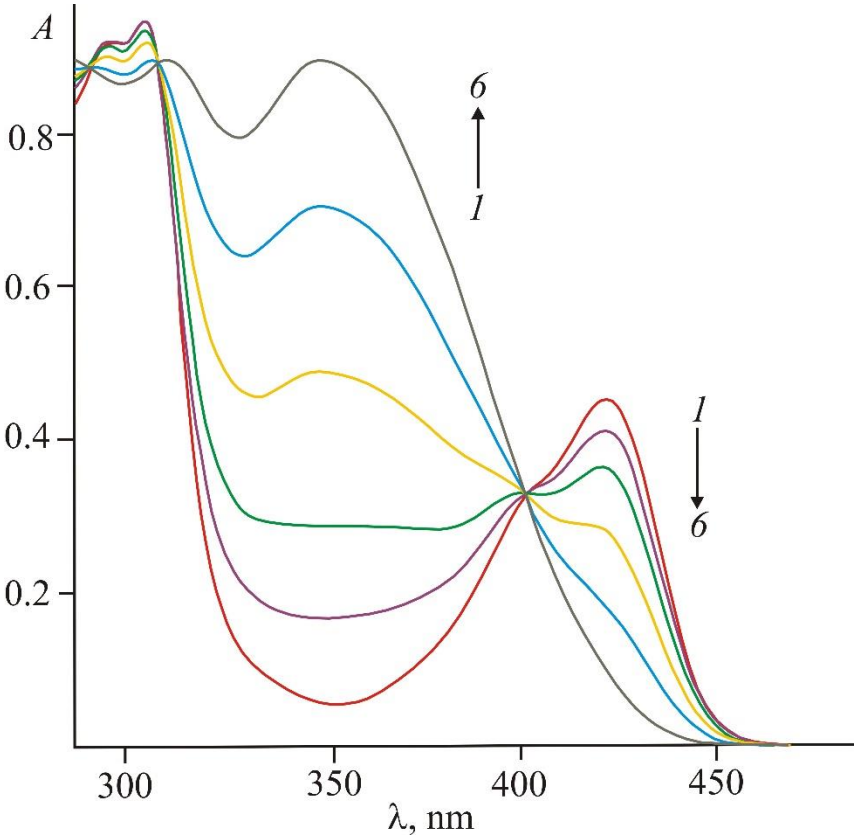

Figure 2: Elecronic absorption spectra of compound **2b** in acetonitrile before (*1*), after 15 s (*2*), 35 s (*3*), 75 s (*4*), 2.5 min (*5*), 5 min (*6*) of irradiation with light 436 nm (*c* 5.0 × 10^{-5} mol L^{-1}).

These spectral transformations are caused by photoinitiated *Z/E* isomerization around the C=C bond and subsequent rapid thermal N→O migration of the acyl group [14] to form stable OAc isomers **3a–c** (Scheme 2). The reverse reaction with restoration of the absorption and fluorescence spectra occurs catalytically in the presence of $HClO_4$.

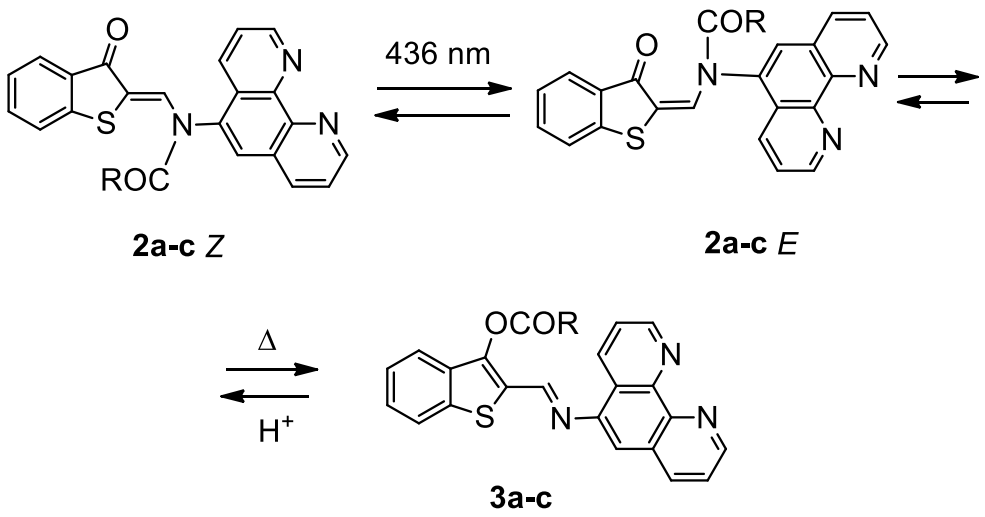

Scheme 2: Photoisomerization of *N*-acylated ketoenamines **2a-c**.

Compounds **3a–c** were isolated preparatively using a modified method we had previously developed using a Sweko IP65 LED emitter [23]. For this purpose, a suspension of yellow solids **2a**, **2b** or **2c** in acetonitrile was boiled for 10–15 s, then irradiated with an emitter for 3–5 min. The procedure was repeated up to 10 times until complete dissolution. Colorless solids of **3a** (80%), **3b** (75%) or **3c** (85%) gradually precipitated. Their structure was confirmed by IR, ^{1}H, ^{13}C NMR spectroscopy and high-resolution mass spectrometry (Supporting Information File 2), as well as by X-ray diffraction analysis.

The molecular structure of **3b** is shown in Figure 3. The crystal data, details of the data collection and refinements for **3b**, complete lists of bond lengths and bond angles are given in Tables S1-S4 (Supporting Information File 3).

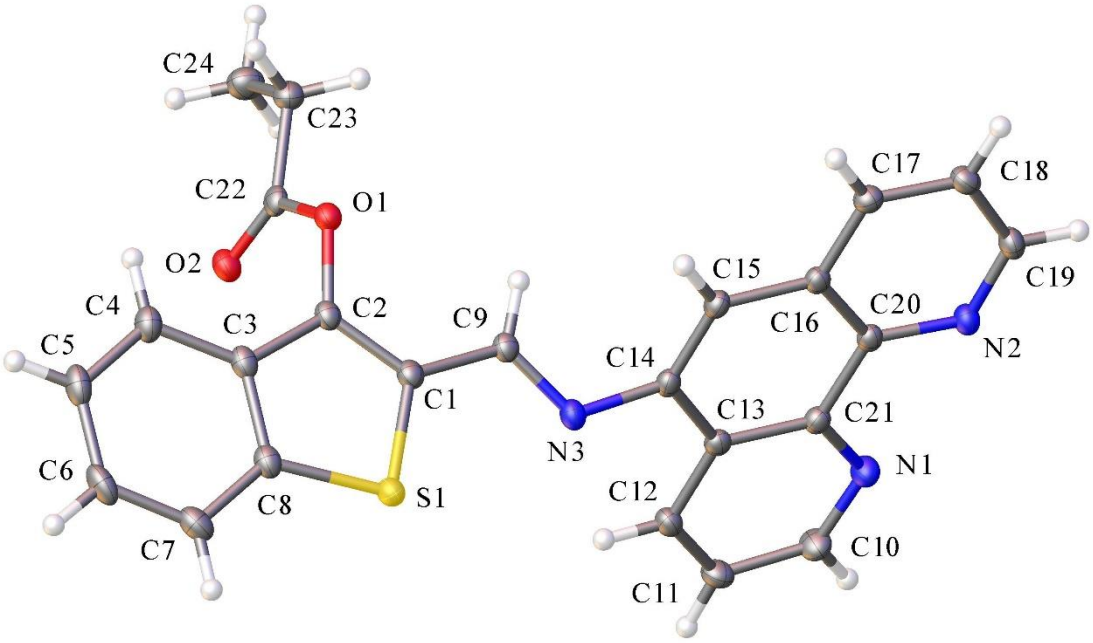

Figure 3: Molecular structure of *O*-acylated isomer **3b.** Thermal ellipsoids are drawn at the 50% probability level.

Compound **3b** has the structure of an *O*-acylated enolimine isomer and possesses a E-S-cis(S,N) conformation relative to the to the C(l)-C(9) bond (Figure 3). The benzothiophene fragment is planar, whereas the propionyl group $COCH_2CH_3$ is not coplanar with this plane. This is due to a torsional rotation around the O(l)-C(2) bond by the angle of C(22)-O(1)-C(2)-C(1) 105.89º. The phenanthroline moiety is planar and rotated relative to the benzothiophene part of the molecule (plane twist angle is 122.73º and fold angle is 4.38º).

The molecular packing of compound **3b** is characterized by the presence of numerous π-π interactions (Figure 4).

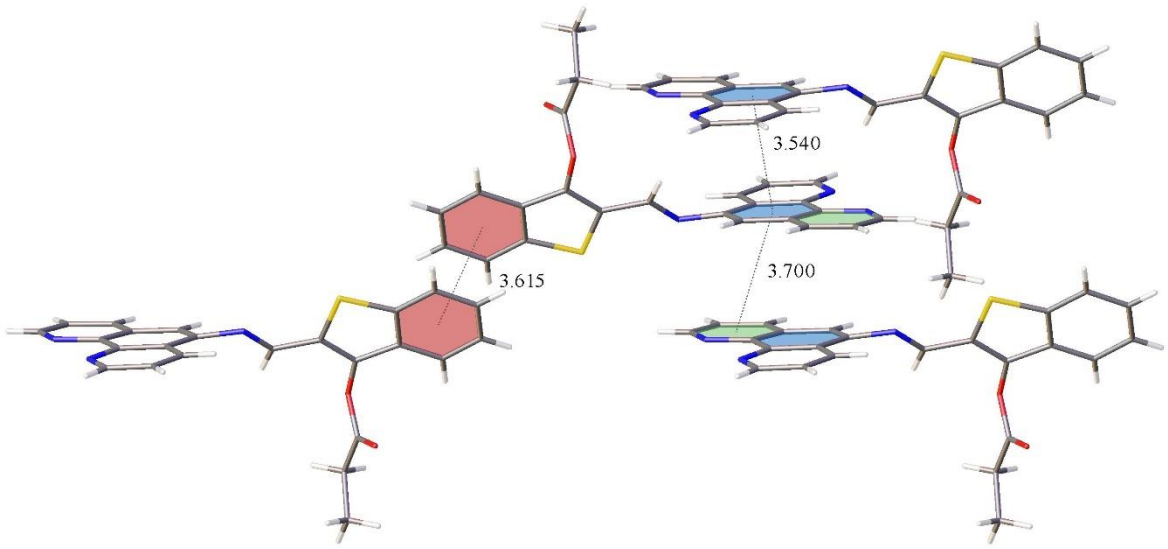

Figure 4: Fragment of the molecular packing of compound **3b**, reflecting the π-π interaction in the crystalline state. The main centroid-centroid distances (Å) are indicated.

The intermolecular interactions in the benzothiophene fragment (red planes in Figure 4) are characterized by the following parameters: plane centroid to plane centroid distance 3.6153(10) Å (shift 1.6063(18) Å, twist and fold angles are 0.0°). The closest contact in the phenanthroline fragment (blue-blue rings, top fragment in Figure 4) has a plane centroid to plane centroid distance 3.5398(9) Å (shift 0.4273(18) Å, twist and fold angles are 0.00°). One of the pyridine cycles of phenanthroline is also involved in a π-π-stacking interaction (blue-green contact in Figure 4) with the plane centroid to plane centroid distance 3.6998(8) Å (plane shift 1.4919(17) Å, twist and fold angle are 1.54° and 1.92°, respectively).

Cation-induced transformations of the absorption and fluorescence spectra of **2a–c** were studied by the action of d-metal perchlorates (Zn^{2+}, Hg^{2+}, Cu^{2+}, Cd^{2+}, Ni^{2+}, Co^{2+} and Fe^{2+}) in acetonitrile (**2a, b**) and DMSO (**2c**). Exclusively Fe^{2+} ions cause an

appearance of a new long-wave broad absorption bands at 480-530 nm with a contrast naked-eye effect - visually distinguishable color change of the solutions from yellow to pink-crimson (Figure 5). Other cations do not demonstrate a measurable effect (Figure 6). Complexes **2a-c** with Fe^{2+} in acetonitrile and DMSO are non-fluorescent.

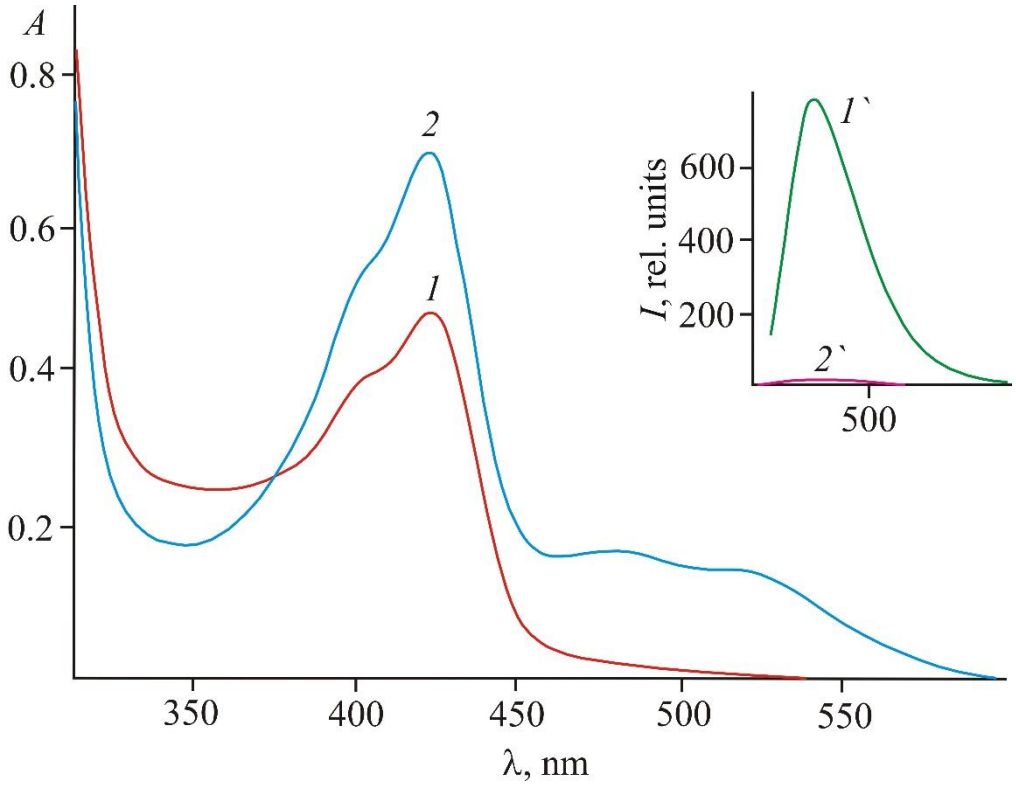

Figure 5: Absorption spectra of compound **2a** in acetonitrile before (*1*) and after the addition of Fe^{2+} cation (*2*) (c_{2a} 5.0 × 10^{-5} mol L^{-1}, $c_{Fe(II)}$ 1.0 × 10^{-4} mol L^{-1}); inset: fluorescence spectra before (*1'*) and after the addition of Fe^{2+} ion (*2'*) (λ_{ex} = 422 nm).

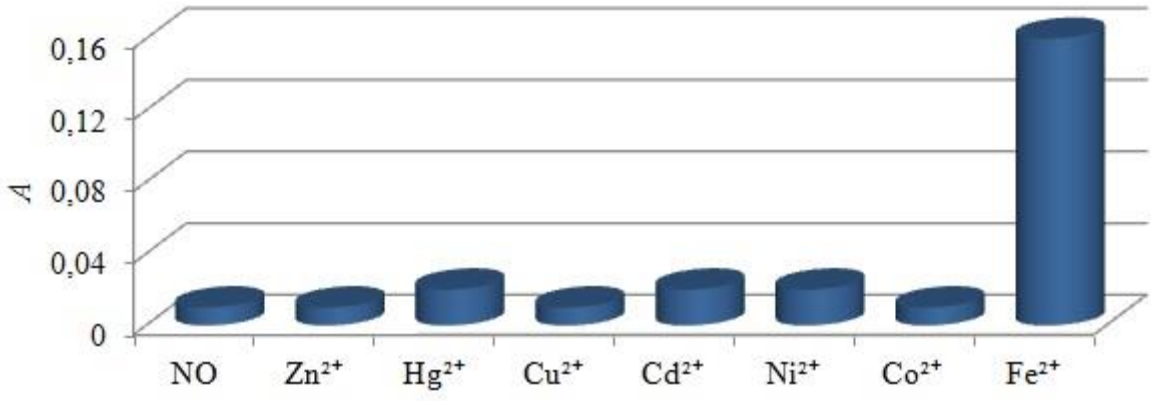

Figure 6: Changes in the absorption intensity of compound **2a** in acetonitrile at 520 nm after the addition of metal perchlorates (c_{2a} 5 × 10^{-5} mol L^{-1}, c_{cat} 1.0 × 10^{-4} mol L^{-1}).

According to the data of spectrophotometric titration and the isomolar series method, compounds **2a-c** form with iron(II) cation complexes **4a-c** with a 2:1 composition (Scheme 3 and Figure 7).

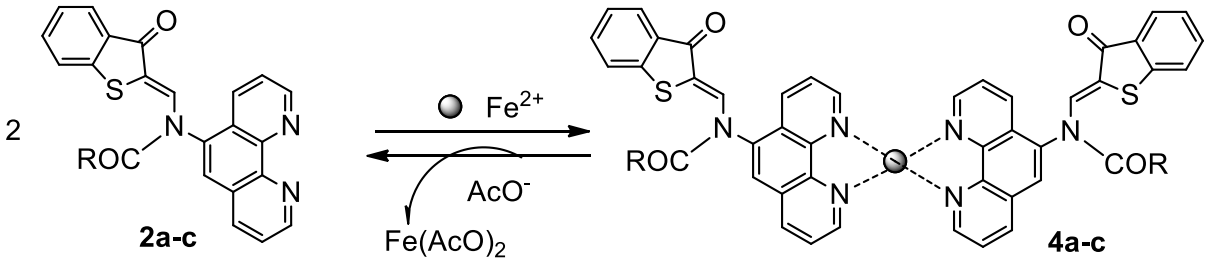

Scheme 3: Sequential interaction of compounds **2a-c** with Fe^{2+} cations and AcO^- anions.

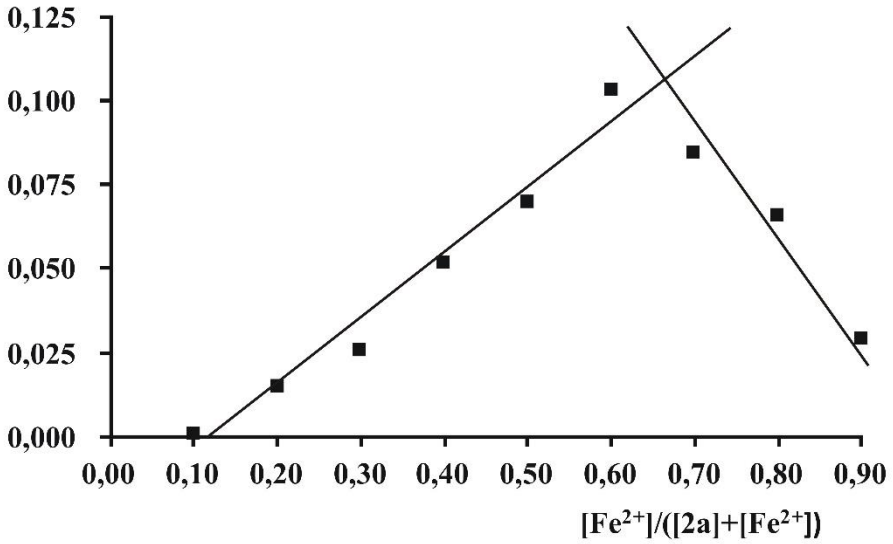

Figure 7: Job's plot at wavelength 429 nm, reflecting the interaction of compound **2a** and Fe^{2+} in acetonitrile. The total concentration [**2a**]+[Fe^{2+}] was 1.5 × 10^{-4} mol L^{-1}.

Selective interaction of the resulting *in situ* complex **4a** with acetate anions was detected, leading to the restoration of the absorption and emission spectra [24,25]. This process can be carried out at least 3-5 times, which allows modulating optical and fluorescent properties by sequentially adding Fe^{2+} and AcO^- ions to an acetonitrile solution of compound **2a**.

Conclusion

Thus, a series of *N*-acylated 2-aminomethylenebenzo[*b*]thiophene-3(2*H*)-ones with terminal phenantroline receptor substituent was synthesized. Upon irradiation with light of 436 nm, the resulting compounds in solutions exhibit negative photochromism due to photoinitiated *Z/E* isomerization around the C=C bond followed by rapid thermal

N→O migration of the acyl group and the formation of *O*-acylated isomers. This rearrangement is accompanied by a decrease of the initial fluorescence intensity at 465-468 nm up to zero, since the resulting OAc form is non-emissive. The reverse reaction occurs catalytically in the presence of $HClO_4$. Special methodics for the preparative isolation of photoproducts has been developed. For the first time, *O*-acylated photoproducts were fully characterized by IR, ^{1}H, ^{13}C NMR spectroscopy, high-resolution mass spectrometry and X-ray diffraction analysis**.** Selectively Fe^{2+} ions cause an appearance of a new long-wave broad absorption bands at 480-530 nm with a contrast naked-eye effect - visually distinguishable color change of the solutions from yellow to pink-crimson. The obtained complexes with Fe^{2+} in acetonitrile and DMSO are non-fluorescent. They selectively interact with acetate anions, which lead to the restoration of initial absorption and emission spectra. Thus, the obtained compounds are dual-mode “on-off-on” switches of fluorescent properties upon sequential exposure to light/H^{+} and sequential addition of Fe^{2+}/AcO^{-} ions.

Experimental

General: The ^{1}H and ^{13}C NMR spectra were recorded on an integrated analytical LC-SPE-NMR-MS system AVANCE-600 (Bruker) (600 MHz, ^{1}H; 150.96 MHz for ^{13}C) in $CDCl_3$. The signals were referred with respect to the signals of residual protons of deutero solvent (7.24 ppm). IR spectra were recorded on an FT/IR-6800 FTIR spectrometer (JASCO). The IR and NMR spectra were recorded using equipment from the Shared Use Centre “Molecular spectroscopy” of the Southern Federal University. Electronic absorption spectra were obtained on a Varian Cary 100 spectrophotometer. Electronic emission spectra were recorded on a Varian Cary Eclipse spectrofluorimeter. Acetonitrile and DMSO (spectral pure grade), cadmium,

mercury(II), copper(II), zinc, nickel(II), cobalt(II), iron(II) perchlorates and tetra-*n*-butylammonium acetate (Aldrich) were used to prepare the solutions. The solutions (in a quartz cell, *l* = 1 cm) were irradiated with filtered light from a high-pressure Hg lamp on a Newport 66,941 equipment supplied with a set of interference light filters. The intensity of light was 6.4×10^{16} photons·s^{-1} for the 436 nm spectral line. For preparative purposes, a Sweko IP65 led emitter (SUL-S1-20W-230-4000K-WH) was used. Spectral-fluorescent experiments were performed using solutions in acetonitrile or DMSO in quartz cells (optical path *l* 1.0 cm, volume *V* 2 mL). Stock solutions of compounds **2a-c** (*c* 1.0×10^{-4} mol L^{-1}) and metal perchlorates (*c* 2.0×10^{-4} mol L^{-1}) were used. 1 mL of **2a-c** solution and 1 mL of perchlorate solution were mixed directly in the cuvette and thoroughly stirred. Hence, working concentration of the compounds **2a-c** and the cations was 5.0×10^{-5} mol $L^{-1}$and 1.0×10^{-5} mol L^{-1}. High resolution mass spectrometry analysis was performed on a Bruker UHR-TOF Maxis™ Impact instrument (electrospray ionization). Melting points were determined on a Fisher-Johns melting point apparatus.

X-ray diffraction study: The X-ray diffraction data set of compound **3b** was recorded on an Agilent SuperNova diffractometer using a microfocus X-ray radiation source with copper anode and Atlas S2 two-dimensional CCD detector. Crystal data for $C_{24}H_{17}N_3O_2S$ (*M* = 411.46 g mol^{-1}): triclinic, space group P-1 (no. 2), *a* = 7.43030(10) Å, *b* = 9.6398(2) Å, *c* = 14.3294(3) Å, *α* = 75.731(2)°, *β* = 82.686(2)°, *γ* = 78.664(2)°, *V* = 971.93(3) $Å^3$, *Z* = 2, *T* = 293(2) K, μ(Cu Kα) = 1.701 mm^{-1}, D_{calc} = 1.406 g/cm^3, 17777 reflections measured (9.61° ≤ 2Θ ≤ 152.768°), 4053 unique (R_{int} = 0.0201, R_{sigma} = 0.0153) that were used in all calculations. The final R_1 was 0.0307 (I > 2σ(I)) and wR_2 was 0.0813 (all data).

Reflections were recorded and unit cell parameters were determined and refined using the dedicated CrysAlisPro software suite [26]. The structure was solved with the ShelXT programme [27] and refined with the ShelXL programme [28], and the graphics were rendered using the Olex2 software suite [29]. The complete X-ray structural data set for compound **2a** was deposited at the Cambridge Crystallographic Data Centre (CCDC 2299603). These data can be obtained free of charge via http://www.ccdc.cam.ac.uk/conts/retrieving.html, or from the Cambridge Crystallographic Data Centre, 12 Union Road, Cambridge CB2 1EZ, UK; fax: (+44) 1223-336-033; or e-mail: deposit@ccdc.cam.ac.uk.

Supporting Information

Supporting Information File 1:

Experimental procedures and characterization data for all novel compounds 1, 2a–c, 3a–c.

Supporting Information File 2:

1H, 13C NMR, IR and HRMS spectra of all novel compounds.

Supporting Information File 3:

X-ray analysis data of 3b.

Funding

This study was financially supported by the Ministry of Science and Higher Education of the Russian Federation in the scope of the State Task in the Field of Science (no. FENW_2023-0020) and in the scope of the State Task to Southern Scientific Centre of the Russian Academy of Sciences (no. 122020100282-6, V.P. Rybalkin and A.D. Dubonosov).

ORCID® iDs

V.P. Rybalkin - https://orcid.org/0000-0001-9327-1472

S.Yu. Zmeeva - https://orcid.org/0000-0002-0428-1087

L.L. Popova - https://orcid.org/0000-0002-9362-8408

I.V. Dubonosova - https://orcid.org/0000-0002-3368-5259

O.Yu. Karlutova - https://orcid.org/0000-0002-3290-101X

O.P. Demidov - https://orcid.org/0000-0002-3586-0487

A.D. Dubonosov - https://orcid.org/0000-0003-4701-2271

V.A. Bren - https://orcid.org/0000-0003-3192-6204

References

1. Pianowski Z. L., Ed.; *Molecular Photoswitches: Chemistry, Properties, and Applications*; Wiley-VCH: Weinheim, 2022.
2. Tian, H.; Zhang, J., Eds.; *Photochromic Materials: Preparation, Properties and*

Applications; Wiley-VCH: Weinheim, 2016.

3. Duerr, H.; Bouas-Laurent, H., Eds.; *Photochromism: Molecules and Systems*, *revised edition*; Elsevier: Amsterdam, 2003.
4. Crano, J. C.; R. Guglielmetti, R. J., Eds.; *Organic Photochromic and Thermochromic Compounds*; Springer: New York, 2002.
5. Fitzmaurice, O.; Bartkowski, M.; Giordani, S. *Front. Chem.* **2022**, *10*, 859450. doi:10.3389/fchem.2022.859450
6. Magri, D. C. *Coord. Chem. Rev.* **2021**, *426*, 213598. doi:10.1016/j.ccr.2020.213598
7. Andréasson, J.; Pischel, U. *Coord. Chem. Rev.* **2021**, *429*, 213695. doi:10.1016/j.ccr.2020.213695
8. Welleman, I. M.; Hoorens, M. W. H.; Feringa, B. L.; Hendrikus, H.; Boersma, H. H.; Szymański W. *Chem. Sci.* **2020**, *11*, 11672-11691. doi:10.1039/d0sc04187d
9. Krämer, J.; Kang, R.; Grimm, L. M.; De Cola, L.; Picchetti, P.; Biedermann, F. *Chem. Rev.* **2022**, *122*, 3459-3636. doi:10.1021/acs.chemrev.1c00746
10. Li, M.; Zhao, J.; Chu, H.; Mi, Y.; Zhou, Z.; Di, Z.; Zhao, M.; Li, L. *Adv. Mater.* **2019**, *31*, 1804745. doi:10.1002/adma.201804745
11. Aiken, S.; Edgar, R. J. L.; Gabbutt, C. D.; Heron, B. M.; Hobson, P. A. *Dyes Pigm.* **2018**, *149*, 92-121. doi:10.1016/j.dyepig.2017.09.057
12. Metelitsa, A.; Chernyshev, A.; Voloshin, N.; Solov'eva, E.; Rostovtseva, I.; Dorogan, I.; Gaeva, E.; Guseva, A. *Dyes Pigm.* **2021**, *186*, 109070. doi:10.1016/j.dyepig.2020.109070
13. Bren, V. A.; Dubonosov, A. D.; Popova, O. S.; Revinskii, Yu. V.; Tikhomirova, K. S.; Minkin, V. I. *Int. J. Photoenergy* **2018**, *2018*, 9746534. doi:10.1155/2018/9746534
14. Minkin, V. I.; Bren, V. A.; Dubonosov, A. D.; Tsukanov, A. V. *Chem. Heterocycl. Compd.* **2012**, *48*, 107-116. doi:10.1007/s10593-012-0974-6

15. Crespi, S.; Simeth, N. A.; Di Donato, M.; Doria, S.; Stindt, C. N.; Hilbers, M. F.; Kiss, F. L.; Toyoda, R.; Wesseling, S.; Buma, W. J.; Feringa, B. L.; Szymanski, W. *Angew. Chem. Int. Ed.* **2021**, *60*, 25290. doi:10.1002/anie.202111748

16. Kobauri, P.; Dekker, F. J., Szymanski, W., Feringa, B. L. *Angew. Chem. Int. Ed.* **2023**, *62*, e202300681. doi:10.1002/anie.202300681

17. Kuntze, K., Pooler, D. R. S.; Di Donato, M.; Hilbers, M. F.; van der Meulen, P.; Buma, W. J.; Priimagi, A.; Feringa, B. L.; Crespi, S. *Chem. Sci.* **2023**, *14,* 8458-8465. doi:10.1039/d3sc03090c

18. Sacherer, M.; Hampel, F.; Dube, H. *Nat. Commun.* **2023**, *14*, 4382. doi:10.1038/s41467-023-39944-x

19. Huang, C.; Hecht, S. *Chem. Eur. J.* **2023**, *29*, e202300981. doi:10.1002/chem.202300981

20. Popova, O. S.; Podshibyakin, V. A.; Shepelenko, E. N.; Kuzmina, L. G.; Zaitsev, S. A.; Dubonosov, A. D.; Bren, V. A.; Minkin, V. I. *J. Mol. Struct.* **2023**, *1272*, 134211. doi:10.1016/j.molstruc.2022.134211

21. Alreja, P., Kaur, N. *RSC Adv.* **2016**, *6*, 23169-23217. doi:10.1039/c6ra00150e

22. Shepelenko, E. N.; Karamov, O. G.; Podshibyakin, V. A.; Revinskii, Yu. V.; Tikhomirova, K. S.; Dubonosov, A. D.; Bren, V. A.; Minkin, V. I. *ARKIVOC* **2017**, No. 5, 196-203. doi:10.24820/ark.5550190.p010.262

23. Rybalkin, V. P.; Zmeeva, S. Yu.; Popova, L. L.; Tkachev, V. V.; Utenyshev, A. N.; Karlutova, O. Yu.; Dubonosov, A. D.; Bren, V. A.; Aldoshin, S. M.; Minkin, V. I. *Beilstein J. Org. Chem.* **2020**, *16*, 1820-1829. doi:10.3762/bjoc.16.149

24. Suganya S.; Naha, S.; Velmathi, S. *ChemistrySelect* **2018**, *3*, 7231-7268. doi: 10.1002/slct.201801222

25. Mukherjee, S.; Talukder, S. *J. Fluoresc.* **2017**, *27*, 1567-1572. doi:10.1007/s10895-016-1974-1

26. CrysAlisPro, Version 1.171.38.41, Rigaku Oxford Diffraction, 2015. https://www.rigaku.com/en/products/smc/crysalis

27. Sheldrick, G. M. *Acta Crystallogr.* **2015**, *C71*, 3-8. doi: 10.1107/S2053273314026370

28. Sheldrick, G. M. *Acta Crystallogr.* **2015**, *A71*, 3-8. doi: 10.1107/S2053229614024218

29. Dolomanov, O. V.; Bourhis, L. J.; Gildea, R. J.; Howard, J. A. K.; Puschmann, H. *J. Appl. Crystallogr.* **2009**, *42*, 339-341. doi:10.1107/S0021889808042726